RSC Advances

ROYAL SOCIETY OF CHEMISTRY

www.rsc.org/advances

Graphical Abstract

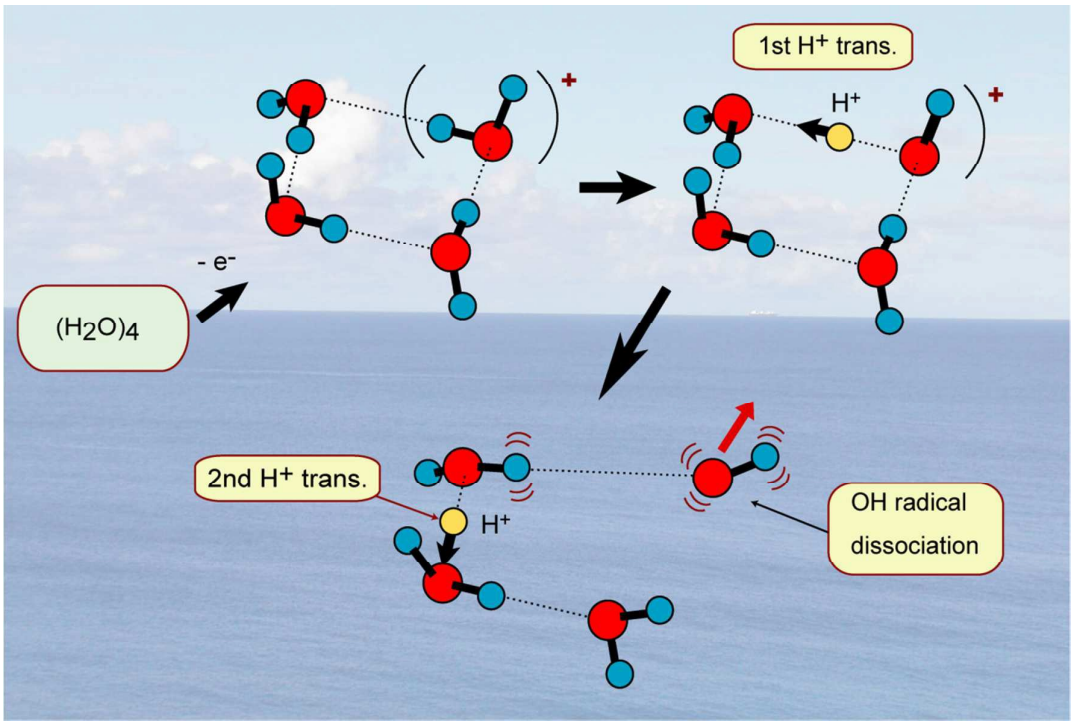

Title: **Proton Transfer Rates in Ionized Water Clusters $(H_2O)_n$ (n=2-4)**

Authors: Hiroto TACHIKAWA*[a] and Tomoya TAKADA[b]

[a]*Division of Materials Chemistry, Graduate School of Engineering, Hokkaido University, Kita-ku, Sapporo 060-8628, Japan*
[b]*Department of Material Chemistry, Asahikawa National College of Technology, Syunkodai, Asahikawa 071-8142, Japan*

Correspondence to:
Dr. Hiroto TACHIKAWA*
Division of Materials Chemistry
Graduate School of Engineering
Hokkaido University
Sapporo 060-8628, JAPAN
hiroto@eng.hokudai.ac.jp
Fax. +81 11706-7897

Proton Transfer Rates in Ionized Water Clusters $(H_2O)_n$ (n=2-4)

Hiroto TACHIKAWA*[a] and Tomoya TAKADA[b]

[a]*Division of Materials Chemistry, Graduate School of Engineering, Hokkaido University, Sapporo 060-8628, Japan*

[b]*Department of Bio- and Material photonics, Chitose Institute of Science and Technology,Chitose 066-8655, Japan*

Abstract: Proton transfer process is usually dominant in several biological phenomena such as an energy relaxation of photo-excited DNA base pair and a charge relay process in Ser-His-Glu. In the present study, the rates of proton transfer along hydrogen bond in water cluster cation have been investigated by means of direct ab-initio molecular dynamics (AIMD) method. Three basic clusters, water dimer, trimer and tetramer, $(H_2O)_n$ (n=2-4), were examined as the hydrogen bonded system. It was found that the rate of the first proton transfer is strongly dependent on the cluster sizes: average time scales of proton transfer for n= 2, 3, and 4 were 28, 15, and 10 fs, respectively, (MP2/6-311++G(d,p) level) suggesting that proton transfer reactions are very fast processes in three clusters. The second proton transfer was found in n=3 and 4 (the average time scales for n=3 and 4 were 120 fs and 40 fs, respectively, after the ionization). The reaction mechanism was discussed on the basis of theoretical results.

Keywords: water cluster; ionization; proton transfer; reaction dynamics; ab initio MD

1. Introduction

It has been predicted that water ice in a comet is not crystal, but amorphous ice:[1-5] namely, the water ice in the comet is close to the aggregation of several sized-water clusters. Hence, in approaching of comet to sun, the water clusters are directly irradiated by cosmic ray from sun light, and the cluster will be ionized.[6-13] Studying the ionization dynamics of water cluster would provide important information on the formation mechanism of ionic species in the comet. Also, a proton transfer process is usually dominant in several biological phenomena such as an energy relaxation of photo-excited DNA base pair[14-19] and charge relay processes in Ser-His-Glu(or Asp) catalytic triads.[20-23]

From experimental points of view, photo-ionization of the water clusters has been investigated by means of several techniques.[24-28] It was found that the reaction occurs as follows:[24,27]

$$(H_2O)_n + Ip \rightarrow [(H_2O)_n^+]_{VER} + e^- \quad \text{(ionization)}$$

$$[(H_2O)_n^+]_{VER} \rightarrow (H_3O^+)(OH)(H_2O)_{n-2} \quad \text{(complex formation)}$$

$$\rightarrow H^+(H_2O)_{n-1} + OH \quad \text{(OH dissociation)}$$

$$\rightarrow H^+(H_2O)_{n-k} + (k-1)H_2O + OH \quad \text{(OH dissociation + } H_2O \text{ evaporation)},$$

where *Ip* and VER mean ionization potential and vertical ionized state from the parent neutral cluster, respectively. Three reaction channels were observed as decay processes of the ionized water clusters. The first channel is the complex formation in which the proton is transferred from H_2O^+ to H_2O, and the long-lived complex composed of the $(H_3O^+)(OH)$ core is formed in the cluster. In the second channel, the OH radical is dissociated from the $(H_2O)_n^+$ ion. The third channel is composed of three-body

dissociation.

Early experiments showed that the parent ion $(H_2O)_n^+$ is observed only for the water dimer (n=2), whereas the protonated water $H^+(H_2O)_m$ (m<n) is observed in the larger clusters. The OH formation was also observed in the larger clusters. The absence of the parent ion is consistently explained in terms of poor Franck-Condon overlaps between the neutral and the ionic states whose potential minima are largely displaced from each other (n=2).[28] Thus, the reaction channels are strongly dependent on the cluster size. In all clusters, the first proton transfer is an important trigger in the decay process of water cluster cation.

In the present study, direct ab-initio molecular dynamics (AIMD) calculation[29,30] was applied systematically to the ionization dynamics of water dimer, trimer and tetramer $(H_2O)_n$ (n=2-4) in order to estimate the reaction rates of the first and second proton transfer processes in the water cluster cation. In previous study,[31] we preliminary investigated the ionization of water clusters $(H_2O)_n$ (n=2-6) using direct AIMD method at the Hartree-Fock (HF) level, and showed that a dissociation of hydroxyl radical (OH) becomes more dominant in the larger clusters. In the present work, we performed the direct AIMD calculation on more accurate potential energy surface (MP2/6-311++G(d,p) level) to estimate the proton transfer rate along the hydrogen bond in the water cluster cation. Especially, the ionization dynamics of water clusters were systematically investigated with the same procedure for n=2-4, and the cluster size dependency of proton transfer rate was compared with each other.

Information on the structures and energetics for water cluster cation has been accumulated from both theoretical[32-43] and experimental points of view. [8-11,51-54] The neutral water dimer has a linear form in its equilibrium structure. The structure of the

cationic state of the water dimer is largely distorted from the neutral one: the structure of $(H_2O)_2^+$ is composed of the H_3O^+ ion and the OH radical, expressed by (H_3O^+OH), where the proton is transferred from H_2O^+ to H_2O following the ionization of $(H_2O)_2$.[12]

Barrnet and Landman searched the stable structure of water cluster cations $(H_2O)_n^+$ (*n*=3-5) using ab-initio calculations.[32] Their calculations showed that the proton transferred complex (H_3O^+OH) exists as a core cation in the clusters for all cation clusters. Recently, the similar feature was reported by Lee and Kim using more accurate theoretical levels.[33] IR spectroscopy observed by Fujii and co-workers indicated that water trimer cation is composed of proton transferred type.[24]

Formation processes of water cluster cation were investigated by several groups. Furuhama et al. applied partitioning method of the kinetic energy to the ionization of water tetramer cation (*n*=4).[34] Recently, Livshits et al. indicated that water pentamer cation causes a proton transfer and OH dissociation.[35] These pictures were also obtained by us.[36] Novakovskaya performed AIMD calculation of $(H_2O)_n^+$ (*n*=4-6).[37] Snapshots of were obtained after the ionization of $(H_2O)_n$ parent clusters. However, she handles only phenomenalism and did not perform the detailed argument about the proton transfer mechanism.

For the water dimer and trimer cations (*n*=2-3), we investigated the ionization dynamics by means of direct AIMD method.[38,39] The water dimer cation has two low-lying electronic states: the ground state (^{2}A" state) and the first excited state (^{2}A' state). From our calculations, it was found that the ionization to the ^{2}A" state gives a proton transferred product (H_3O^+-OH), whereas that to the ^{2}A' state gives hydrazine-like complex. Thus, the static structures and limited reaction dynamics calculations were carried out for $(H_2O)_n^+$. There is no detailed analysis for the rate of proton transfer in

water cluster cation.

2. Method of calculation

Static ab-initio calculations were carried out using Gaussian 09 program package using 6-311++G(d,p) basis sets.[40] The geometries and energies were obtained by MP2, QCISD and CCSD(T) methods. The atomic charge was calculated by means of natural population analysis (NPA) method.

In the direct AIMD calculation,[41,42] first, the geometry of neutral clusters $(H_2O)_n$ was fully optimized at the MP2/6-311++G(d,p) level. The trajectory on the ionic state potential energy surface of $(H_2O)_n^+$ was started from the equilibrium point of parent neutral cluster. The velocities of all atoms and angular momenta were set to zero at time zero in the trajectory calculation. Also, temperature of the system and excess energy from the potential energy surface at time zero were fixed to 0 K and zero, respectively. The equation of motion was solved by the velocity Verlet algorithm[43] with a time step of 0.05 fs. We checked carefully that the drift of total energy (= potential energy plus kinetic energy) is less than 0.05 kcal/mol in all trajectories. No symmetry restriction was applied to the calculation of the energy gradients.

The relation of total, potential and kinetic energies is expressed by

$$E(toal) = E(kinetic) + E(potential)$$

Since we used the microcanonical ensemble (NVE ensemble) in the AIMD calculation, the total energy of the reaction system is constant during the MD simulation. Instead, the potential and kinetic energies largely vibrate as a function of time. For example, the relation of these energies for a sample trajectory are plotted in Figure S1 (supporting information). Total energy was constant during the reaction.

In addition to the trajectory from the equilibrium point, the trajectories around the equilibrium points were run. A total of ten trajectories were run in each cluster. The selected geometries on Franck-Condon region were chosen as follows: first, the structure of $(H_2O)_n$ (n=2-4) was fully optimized at the MP2/6-311++G(d,p) level of theory. The total energy and optimized structure of $(H_2O)_n$ (n=2-4) are expressed by $E_0(n)$ and $[(H_2O)_n]_0$, respectively. Second, the geometries of $(H_2O)_n$ (n=2-4) were randomly generated around the equilibrium points of $[(H_2O)_n]_0$. The generated geometry is expressed by $[(H_2O)_n]_i$, and total energy is expressed by $E_i(n)$, where notation $\boldsymbol{i}$ is number of generated configurations of $[(H_2O)_n]_i$. Third, the energy difference of E_i from E_0 was calculated as $\Delta E_i = E_i - E_0$. We selected the generated geometry with ΔE_i less than 1.0 kcal/mol ($\Delta E_i < 1.0$ kcal/mol). The direct AIMD calculations were started from the selected geometries. The trajectory calculations of $(H_2O)_n^+$ were performed under constant total energy condition at the MP2/6-311++G(d,p) level.

In addition to the MP2 geometries of $(H_2O)_n$, the optimized structures obtained by QCISD/6-311++G(d,p) and CCSD/6-311++G(d,p) were examined as starting geometries of $[(H_2O)_n^+]_{ver}$ in the direct AIMD calculations to check the effects of initial geometry on the proton transfer rate.

3. Results

A. Structures of the water clusters.

The optimized structures of the water clusters $(H_2O)_n$ (n=2-4) are illustrated in Figure 1. The water dimer (n=2) has a typical linear form with a distance of hydrogen bond of 1.966 Å at the CCSD/6-311++G(d,p) level. The O-O bond distance was 2.928 Å. This structure is in reasonably agreement with experiment (distance of hydrogen

bond is 2.019 Å).[66] In case of water trimer (*n*=3), all water molecules were located under different environment. The distances of hydrogen bonds were 1.952 Å (W1-W2) and 1.950 Å (W2-W3). The oxygen-oxygen distance in W1-W3 was 2.834 Å. In the water tetramer (*n*=4), the distance of hydrogen bond was significantly shortened as r(O--HO)=1.830 Å relative to those of *n*=2 and 3 (1.966 and 1.950 Å). The similar geometrical features of $(H_2O)_n$ (*n*=2-4) were obtained at the MP2/6-311++G(d,p) level: the distances of hydrogen bond for *n*=2, 3, and 4 were calculated to be 1.951, 1.917, and 1.791 Å, respectively.

The molecular charges on the water molecules obtained by the natural population analysis (NPA) are given in Table 1. In water dimer, charges on W1 and W2 were +0.02 and -0.02, meaning that the charge is slightly separated in the dimer. On the other hand, the charges on all water molecules in $(H_2O)_n$ (*n*=3 and 4) were close to zero. At the vertical ionization states, charge distribution was largely changed: a positive charge and spin density were mainly localized on only one water molecule in each cluster cation. In vertical ionized state, $[(H_2O)_2^+]_{ver}$, the charge distribution on W1 and W2 were 0.95 and 0.05, respectively, where W1 and W2 are proton donor and acceptor water molecules, respectively. The spin density was localized on the proton donor in water dimer. This is due to the fact that highest occupied molecular orbital (HOMO) of water dimer is non-bonding orbital of the proton donor (See, Figure S2 in supporting information).

The molecular charges in $[(H_2O)_3^+]_{ver}$, were 0.91 (W1), 0.07(W2), and 0.02 (W3). Each water molecule was located in different environment (See, Figure S3 in supporting information). The charges on W1, W2, W3, and W4 of $[(H_2O)_4^+]_{ver}$ are +0.89, +0.08, +0.03, and +0.01, respectively, at the MP2/6-311++G(d,p) level, indicating that the hole is mainly localized on W1. This is due to the fact that the structure of $(H_2O)_4$ was

calculated without symmetry restriction. Hence, each water molecule was located in different environment. The spatial distribution of spin density is illustrated in Figure 1, indicating that the unpaired electron is mainly localized on one water molecule (W1), although a part of spin densities is distributed on W4. The similar features were obtained for $[(H_2O)_n^+]$ (n=2 and 3).

B. Ionization dynamics of water trimer (n=3)

Ionization processes of n=2 and 3 from the optimized structures were already discussed in our previous papers.[38,39] Hence, the results are briefly given in this section. The direct AIMD calculation for the n=2 gave the proton transferred product: $[(H_2O)_2^+]_{ver} \rightarrow H_3O^+(OH)$. The calculation for the n=3 gave two reaction channels for the decay process of $[(H_2O)_3^+]_{ver}$: these are the OH dissociation and complex formation channels. The former was main channel in n=3. Here, the results of the dissociation channel are described in briefly.

Snapshots for the dissociation channel where the OH radical leaves from the system are illustrated in Figure 2. The position of proton of W1 (H1) is located at r_1=1.895 and r_2=0.977 Å at time zero (point a). The oxygen-oxygen distance is R_{12}= 2.781 Å. After the ionization, the hole is mainly localized on one of the water molecules (W1) in the water trimer cation. The proton of $W1^+$ was immediately transferred to W2: the distances of proton were r_1=1.046 Å and r_2=1.651 Å at time =12 fs (point b), and the ion-radical pair $(H_3O^+)OH$ is formed within very short time period (time= 12 fs at point b). The process of this proton transfer is the same as that of complex channel. In addition to the first proton transfer from $W1^+$ to W2, the second proton transfer takes place in the OH dissociation channel. This process occurs from the protonated W2 (i.e.,

H_3O^+) to W3 around 100 fs. Figure 2(c) shows that the proton transfer takes place from H_3O^+ to W3 at 100 fs. After the second proton transfer, the OH radical was fully separated from the H_3O^+ ion and was dissociated from W2. The OH radical leaved gradually from the system and reached to R_{12}=4.501 Å at 250 fs (product d). Final product was $H_2O(H_3O^+)$ + OH in this trajectory.

C. Ionization dynamics of water tetramer (*n*=4)

Snapshots of $(H_2O)_4^+$ following vertical ionization of neutral water tetramer with the cyclic form are illustrated in Figure 3. At time zero, the spin densities on W1, W2, W3, and W4 were 0.99, 0.01, 0.00, and 0.00, respectively, indicating that a hole was localized on W1. The distances of r_1 and r_2 were 0.977 and 1.791 Å, respectively. After the ionization, a proton of W_1^+ was rapidly transferred to W2. The positions of proton were (r_1=1.436 Å and r_2=1.303 Å at 7 fs), and (r_1=1.787 Å and r_2= 0.950 Å at 12 fs). This result indicates that the first proton transfer takes place within 12 fs after the ionization. The oxygen-oxygen distances of W1-W2 were 2.749 Å (time zero), 2.766 Å (7 fs) and 2.791 Å (12 fs), indicating that only the proton is transferred under the fixed dimer structure. The next specific point is that W4 leaves gradually from $W1^+$ due to the repulsive interaction between the proton of W4 and a positive charge of $W1^+$ (indicated by the arrow at 7 fs).

The second proton transfer occurred at 37 fs. The snapshot at 53 fs (point **d**) shows that the proton is located at the middle of W2 and W3 (r_3=1.146 Å and r_4=1.167 Å). This structure corresponds to the Zundel-like complex, indicating that the second proton transfer takes place via the Zundel-like complex. At 82 fs (point **e**), the H_3O^+(W3) ion was completely formed (r_3=1.727 Å and r_4=1.008 Å), and the attractive interaction

between OH radical and H_3O^+ was disappeared by the separation by the H_2O molecule (W2 at 82 fs). Hence, the OH radical was rapidly dissociated from W2. Finally, the solvated H_3O^+ ion was remained in the reaction system (128 fs).

Potential energy

The time evolution of potential energy of the system is given in Figure 4. The zero level of the energy corresponds to that of $[(H_2O)_4^+]_{VER}$ at vertical ionized point from the neutral tetramer (point a). The potential energy decreased rapidly to -20 kcal/mol (7 fs) and -40 kcal/mol (12 fs) following the ionization of $(H_2O)_4$. This energy lowering is caused by the first proton transfer from $W1^+$ to W2. The position of proton of $W1^+$ was drastically changed as a function of time: the distance of the transferred proton from the oxygen of W1 was varied from r_1= 1.80 Å to 0.95 Å within 0-12 fs. The potential energy reaches the minimum point at 12 fs (point **c**). Immediately, the energy increased suddenly due to the collision of the proton with the oxygen atom of W2. The oxygen-proton distance (=r_1) vibrated periodically. This result indicates that the transferred proton binds directly to the oxygen atom of W2 after the ionization. Time propagation of R_{OO} was slowly changed, indicating that only proton of $W1^+$ moves rapidly from $W1^+$ to W2. The second proton transfer takes place at 37 fs (=r_2). Once the second proton transfer is completed, the OH radical is dissociated from the system. The distance of OH radical was 3.4 Å at 120 fs.

Reaction rates of proton transfer in water cluster cation (n=4)

Time of proton transfer for *n*=4 is plotted in Figure 5. The results of ten trajectories are given. In addition to the MP2 geometries of $(H_2O)_n$, the optimized structures obtained by QCISD/6-311++G(d,p) and CCSD/6-311++G(d,p) were examined as

starting geometries of $[(H_2O)_n^+]_{ver}$ in the direct AIMD calculations to check the effects of initial geometry on the proton transfer rate.

Time of first proton transfer ($W1^+ \rightarrow W2$) was distributed in the range 9.3-10.7 fs, and average value was 9.9 fs. This is a very fast process. The second proton transfer occurred at 40 fs after the ionization. This is a slow process. The third proton transfer occurred from $W3^+$ to W2 (the reverse proton transfer). Time scales between first and second proton transfer processes are significantly different from each other (ca.10 fs for the first proton transfer vs. ca.40 fs for 2nd proton transfer). This is due to the fact that the first proton transfer proceeds as an extho-thermic reaction: $H_2O^+(W1) + H_2O(W2) \rightarrow OH(W1) + H_3O^+(W2)$. On the other hand, the second proton transfer is iso-thermic reaction: $H_3O^+ (W2) + H_2O(W3) \rightarrow H_2O(W2) + H_3O^+(W3)$. This is an origin of difference of time scales.

The similar analysis was carried out for *n*=2-3, and the results are summarized in Table 2. In *n*=2, only first proton transfer was found as $W1^+ \rightarrow W2$. Average time of the first proton transfer was 28.4 fs. In case of *n*=3, the second proton transfer occurred around 120 fs after the ionization, which is much slower than that of *n*=4.

The first, second and third proton transfer rates obtained by MP4SDQ and CCSD geometries were 9.6 fs (9.6 fs) , 40.7 fs (39.9 fs), and 51.9 fs (49.4 fs), respectively, where the CCSD values are given in the parenthesis. These values are in good agreement with MP2 values. Therefore, the present results are general in water tetramer cation.

D. Structures of radical cation $(H_2O)_n^+$ (*n*=2-4)

The optimized structures of water dimer and trimer radical cations were fully optimized at the MP2/6-311++G(d,p) level of theory. The optimized structures are illustrated in Figure 6. The proton transferred complex was obtained for *n*=2. The radical cation of *n*=3 was composed of H_3O^+, OH radical and H_2O. The H_3O^+ radical cation interacts directly with the OH radical and is solvated by a water molecule. The H_3O^+ radical is located in the center of the complex, and an ion-radical contact pair, (H_3O^+-OH), is formed. These results are consistent with recent works.[44-66]

The radical cation of water tetramer has several conformers. We found five structures of $(H_2O)_4^+$. Among them, four stable structures are illustrated in Figure 6. The most stable structure is complex **1** where the H_3O^+ ion interacts directly with the OH radical and is solvated by two water molecules. In complexes **2** and **3**, the OH radical is separated from the H_3O^+ ion by water molecule. Both complexes **2** and **3** are 2.5 kcal/mol higher in energy than complex **1**. In complex **4**, the H_3O^+ ion interacts directly with the OH radical and is solvated by one water molecule. This complex is 5.1 kcal/mol unstable than complex **1**.

Relative energies of stationary points for *n*=4 are given in Table 3, and the energy diagram for the ionization process of water cluster is illustrated in Figure 7. In case of *n*=4, the radical cation of $(H_2O)_4^+$ was 55.4 kcal/mol lower in energy than the vertical ionization point (ΔE_{stable}). The energy level of OH dissociation channel is 7.9 kcal/mol higher than that of radical cation $(H_2O)_4^+$, indicating that the OH dissociation takes place easily from the radical cation. The available energy of OH dissociation channel (ΔE_{avail}) was 47.5 kcal/mol. The OH dissociation reaction is exthothermic in energy. The available energies for *n*=2 and 3 were calculated to be -0.8 and 15.3 kcal/mol, which are significantly smaller than that of *n*=4. This result indicates that the OH dissociation

occurs easily in *n*=4.

It is noted that the MP2 values are in good agreement with the CCSD values, as shown in Table 3. This fact suggests that the MP2/6-311++G(d,p) calculation would be enough to represent the potential energy surface of water cluster cation.

E. Effects of temperature on the reaction dynamics

In actual water cluster in the comet, the structure is fluctuated around its equilibrium point owing to thermal activation. The effects of temperature on the ionization dynamics were examined in this section. Time evolution of oxygen-oxygen (O-O) bond distances of $(H_2O)_4$ are plotted in Figure 9 as a function of time. Simulations were carried out at 10 K which corresponds to that of molecule in cold interstellar space.[68] The O-O distances were fluctuated in the range 2.70-2.76 A. Eleven geometries of $(H_2O)_4$ were randomly selected, and direct AIMD calculations were carried out at the MP2/6-311++G(d,p) level. The average rates for the first and second proton transfer were calculated to be 9.2 and 40.1 fs, respectively (See, supporting information. All results are given in Figure S4). The corresponding values at zero temperature were 9.9 fs (first proton transfer) and 39.6 fs (second). There were few effects of the temperature on the proton transfer rate. This is due to the fact that 10 K is very low temperature as the thermal activation energy. If the simulation temperature becomes higher (for example, room temperature), the rate of proton transfer will be slow owing to the randomized orientation.

4. Discussion

The present calculations showed that the reaction rates of the first proton transfer are

strongly dependent on the cluster size in *n*=2-4. The average rates were calculated in the order of v(*n*=2) < v(*n* =3) < v(*n* =4). The difference in the reaction rate is caused by the approaching time between $W1^+$ to W2. The distances of hydrogen bond in $(H_2O)_n$ of *n*=2, 3, and 4 are 1.951, 1.917, and 1.791 A, respectively. This difference causes the cluster size dependence of proton transfer rate in $(H_2O)_n$ (*n*=2-4) cluster.

Snapshots of the first proton transfer process from $W1^+$ to W2 are superimposed in Figure 8(left). These snapshots were calculated from direct AIMD calculations of $(H_2O)_4^+$ from the optimized structure of neutral state. The proton was rapidly transferred within 10 fs, and the change of position was significantly large. On the other hand, the positions of the other atoms were hardly changed. Figure 8(right) shows potential energy curve (static ab-initio calculation) plotted along the proton transfer coordinate (*R*) together with potential energy of the system obtained by direct AIMD calculation. The shape of the curve indicates that the proton transfer takes place without activation barrier, and the reactant can reach smoothly to the proton transferred product. The potential energies of AIMD was always lower than PEC, indicating that the structural relaxation of the other geometrical parameter affect slightly to the stabilization of the system.

On the basis of the present calculations, a reaction model of ionization of cyclic water tetramer is proposed. The reactions following the ionization of the water tetramer is summarized as follows:

$$(H_2O)_4 + Ip \rightarrow [(H_2O)_4^+]_{VER} + e^- \quad (1)$$

$$[(H_2O)_4^+]_{VER} \rightarrow (H_2O)_2\text{--}(H_3O^+)\text{-}(OH) \text{ complex} \quad (2)$$

$$\rightarrow (H_2O)\,(H_2O\text{-}H_3O^+) + OH \text{ dissociation} \quad (3).$$

Two reaction channels (complex and OH dissociation) were found from the direct AIMD calculations. By the ionization of water tetramer, a hole is localized on one of the water molecules in $(H_2O)_4$. In case of cyclic form, a proton is rapidly transferred from $H_2O^+(W1^+)$ to H_2O (W2) along the hydrogen bond. Time scale of the proton transfer is about 10 fs (very fast process). Next, the second proton transfer occurred from $W2(H^+)$ to W3 with a time scale of 50-100 fs. The second proton transfer makes the separation of OH from H_3O^+ such as a configuration of H_3O^+-- H_2O--OH. When the separation is completed, the attractive interaction between H_3O^+ and OH is vanished by the H_2O located in the middle of H_3O^+ and OH radical. Immediately, the OH radical is dissociated from the system.

Acknowledgment. The author acknowledges partial support from JSPS KAKENHI Grant Number 24550001 and MEXT KAKENHI Grant Number 25108004.

References

(1) Kouchi, A.; Yamamoto, T.; Kozasa, T.; Kuroda,T.; Greenberg, J., Astron. Astrophys., 1994, 290, 1009–1018.

(2) Yokochi, R.; Marboeuf, U.; Quirico, E.; Schmitt, B., ICARUS, 2012, 218, 760-770.

(3) Molano, GC.; Kamp, I., Astron. Astrophys.,2012, 537, A138.

(4) Gudipati, M.S.; Allamandola, L.J., Astrophys. J., 2003, 596, L195–L198.

(5) Ciesla, F.J., Astrophys. J., 2014, 784, L1.

(6) Gardeinier, G.H.; Johnson, M. ; McCoy, A.B., J. Phys. Chem. A, 2009, 113, 4772.

(7) Soloveichik, P.; O'Donnell, B.A.; Lester, M.; Francisco, J.S.; McCoy, A.B., J. Phys. Chem. A, 2010, 114, 1529-1538.

(8) Douberly, G.E.; Walters, R.S.; Cui, J.; Jordan, K.D.; Duncan, M.A., J. Phys. Chem. A, 2010, 114, 4570-4579.

(9) Guasco, T.L.; Johnson, M.A.; McCoy, A.B., J. Phys. Chem. A, 2011, 115, 5847-5858.

(10) McCunn, L.R.; Roscioli, J.R.; Elliott, B.M.; Johnson, M.A.; McCoy, A.B., J. Phys. Chem. A, 2008, 112, 6074-6078.

(11) Diken, E.G.; Headrick, J.M.; Roscioli, J.R.; Bopp, J.C.; Johnson, M.A.; McCoy, A.B., J. Phys. Chem. A, 2005, 109, 1487-1490.

(12) Vaida, V., J. Chem. Phys., 2011, 135, 020901.

(13) Miller, Y.; Thomas, J.L.; Kemp, D.D.; Finlayson-Pitts, B.J.; Gordon, M.S.; Tobias, D.J.; Gerber, R.B., J. Phys. Chem. A, 2009, 113, 12805–12814.

(14) Chen, X.B.; Fang, W.H.; Wang, H.B., Phys. Chem. Chem. Phys., 2014, 16, 4210-4219.

(15) Greve, C.; Elsaesser, T., J. Phys. Chem. B 2013, 117, 14009−14017.

(16) Brazard, J.; Thazhathveetil, AK.; Vaya, I.; Lewis, FD.; Gustavsson, T.; Markovitsi, D., Photochem. Photobiol. Sci., 2011,10, 175-177.

(17) A. L. Sobolewski, W. Domcke and C. Hattig, Proc. Natl. Acad. Sci. U. S. A., 2005, 102, 17903–17906.

(18) Abo-Riziq, A.; Grace, L.; Nir, EM.; Kabelac. M.; Hobza. P.; de Vries, M., Proc. Natl. Acad. Sci. U. S. A., 2005, 102, 20–23.

(19) Kina, D.; Nakayama, A.; Noro, T.; Taketsugu, T.; Gordon, M.S., J. Phys. Chem. A 2008, 112. 9675-9683.

(20) Zhao, Y.; Chen, NH.; Wu, R.B.; Cao, Z.X., Phys.Chem.Chem.Phys., 2014, 16, 18406-18417.

(21) Buller, A.R.; Townsend, C.A., Proc Natl Acad Sci., 2013; 110, E653–E661.

(22) Ruzzini, A.C.; Bhowmik, S.; Ghosh, S.; Yam, K.C.; Bolin, J.T.; Eltis, L.D., Biochem. 2013, 52, 7428-7438.

(23) Huang, Y.; Lu, Z.; Liu, N.; Chen, YJ., Biocheme., 2012, 94, 471-478.

(24) Mizuse, K.; Kuo, J.L.; Fujii, A., Chem. Science, 2011, 2, 868-876.

(25) Shinohara, H.; Nishi, N.; Washida, N., J. Chem. Phys., 1986, 84, 5561-5567.

(26) Shiromaru, H.; Achiba, Y.; Kimura, K.; Lee, Y.T., J. Phys. Chem., 1987, 91, 17-19.

(27) Shiromaru, H.; Shinohara, H.; Washida, N.; Yoo, H.S.; Kimura, K., Chem. Phys. Lett., 1987, 141, 7-11.

(28) Shiromaru, H.; Suzuki, H.; Sato, H.; Nagaoka, S.; Kimura, K., J. Phys. Chem., 1989, 93, 1832-1835.

(29) Tachikawa, H.; Orr-Ewing, A., J. Phys. Chem. A, 2008, 112, 11575-11581.

(30) Tachikawa, H., J. Phys. Chem. A, 2014, 118, 3230-3236.

(31) Tachikawa, H., J. Phys. Chem. A 2002, 106, 6915-6921.

(32) Barnett, RN; Landman, U., J. Phys. Chem. A,1997, 101, 164-169.

(33) Lee, H.M.; Kim, K.S., J. Chem. Theor. Comput., 2009, 5, 976-981.

(34) Furuhama, A.; Dupuis, M.; Hirao, K., Phys. Chem. Chem. Phys. 2008, 10, 2033-2042.

(35) Livshits, E.; Granot, R.S.; Baer, R., J. Phys. Chem. A, 2011, 115, 5735-5744.

(36) Tachikawa, H., J. Phys. Chem. A 2004, 108, 7853-7862.

(37) Novakovskaya, Y.V., Int. J. Quant. Chem., 2007, 107, 2763-2780.

(38) Tachikawa, H., Phys. Chem. Chem. Phys., 2011, 13, 11206-11212.

(39) Tachikawa, H. and Takada, T., Chem. Phys., 2013, 415, 76.

(40) M. J. Frisch, G. W. Trucks, H. B. Schlegel, G. E. Scuseria, M. A. Robb, J. R. Cheeseman, G. Scalmani, V. Barone, B. Mennucci, G. A. Petersson, H. Nakatsuji, M. Caricato, X. Li, H. P. Hratchian, A. F. Izmaylov, J. Bloino, G. Zheng, J. L. Sonnenberg, M. Hada, M. Ehara, K. Toyota, R. Fukuda, J. Hasegawa, M. Ishida, T. Nakajima, Y. Honda, O. Kitao, H. Nakai, T. Vreven, J. A. Montgomery, Jr., J. E. Peralta, F. Ogliaro, M. Bearpark, J. J. Heyd, E. Brothers, K. N. Kudin, V. N. Staroverov, R. Kobayashi, J. Normand, K. Raghavachari, A. Rendell, J. C. Burant, S. S. Iyengar, J. Tomasi, M. Cossi, N. Rega, J. M. Millam, M. Klene, J. E. Knox, J. B. Cross, V. Bakken, C. Adamo, J. Jaramillo, R. Gomperts, R. E. Stratmann, O. Yazyev, A. J. Austin, R. Cammi, C. Pomelli, J. W. Ochterski, R. L. Martin, K. Morokuma, V. G. Zakrzewski, G. A. Voth, P. Salvador, J. J. Dannenberg, S. Dapprich, A. D. Daniels, O. Farkas, J. B. Foresman, J. V. Ortiz, J. Cioslowski and D. J. Fox, Gaussian 09, Revision A.02, Gaussian, Inc., Wallingford CT, 2009.

(41) Tachikawa, H.; Fukuzumi, T., Phys. Chem. Chem. Phys., 2011, 13, 5881-5887.

(42) Tachikawa, H., Chem. Phys. Lett., 2011, 513, 94-98.

(43) Swope, W.C.; Andersen, H.C. ; Berens, P.H. ; Wilson, K.R., J. Chem. Phys., 1982, 76, 648.

(44) Liu, H.T.; Muller, J.P.; Beutler, M.; Ghotbi, M.; Noack, F.; Radloff, W.; Zhavoronkov, N.; Schulz, C.P.; Hertel, I.V., J. Chem. Phys. 2011, 134, 094305-094310.

(45) Pan, P.-R.; Lin, Y.-S.; Tsai, M.-K.; Kuo, J.-L.; Chai, J.-D., Phys. Chem. Chem. Phys., 2012, 14, 10705–10712.

(46) Tsai, M.-K.; Kuo, J.-L.; Lu, J.-M., Phys. Chem. Chem. Phys., 2012, 14, 13402–13408.

(47) Svoboda, O.; Hollas, D.; Oncak, M.; Slavicek, P., Phys. Chem. Chem. Phys., 2013, 15, 11531-11542.

(48) Do, H.; Besley, N.A., J. Phys. Chem. A, 2013, 117, 5385–5391.

(49) Lu, E-P.; Pan, P-R..; Li, Y-C.; Tsai, M-K.; Kuo, J-L., Phys. Chem. Chem. Phys.,2014, 16, 18888-18895.

(50) Lv, Z-L.; Xu, K.; Cheng,Y.; Chen, X-R., Cai, L-C, J. Chem. Phys., 2014, 141, 054309.

(51) Kamarchik, E.; Kostko, O.; Bowman, J.M.; Ahmed, M.; Krylov, A.I., J. Chem. Phys., 2010, 132, 194311.

(52) Mizuse, K.; Mikami, N.; Fujii, A., Angew. Chem., Int. Ed., 2010, 49, 10119–10122.

(53) Mizuse, K.; Fujii, A., Phys. Chem. Chem. Phys., 2011, 13, 7129–7135.

(54) Mizuse, K.; Fujii, A., Chem. Phys., 2013, 419, 2–7.

(55) Mizuse, K.; Fujii, A., J. Phys. Chem. A, 2013, 117, 929–938.

(56) Sheu, W.S.; Chiou, M.F., J. Phys. Chem. A, 2011, 115, 99.

(57) Livshits, E.; Granot, R. S.; Baer, R., J. Phys. Chem. A, 2011, 115, 5735-5744.

(58) Golan, A.; Ahmed, M., J. Phys. Chem. Lett., 2012, 3, 458-462.

(59) Shields, R.M; Temelso, B.; Archer, K.A.; Morrell, T.E.; Shields, G.C., J. Phys. Chem. A, 2010, 114, 11725-11737.

(60) Kaledin, M.; Wood, C.A., J. Chem. Theor. Comput., 2010, 6, 2525-2535.

(61) Wang, Y.M.; Bowman, J.M., J. Chem.Phys., 2011, 135, 131101.

(62) Lee, H.M.; Kim, K.S., Theor. Chem. Acc. 2011, 130, 543-548.

(63) Ceponkus, J.; Uvdal, P.; Nelander, B., J. Chem. Phys., 2011, 134, 064309.

(64) Pincua, M.; Gerber, R.B., Chem. Phys. Lett., 2012, 531, 52-58.

(65) Jieli, M.; Aida, M.,J. Phys. Chem. A, 2009, 113, 1586–1594.

(66) Hammer, N.I.; Roscioli, J.R.; Johnson, M.A., J. Phys. Chem. A, 2005, 109, 7896–7901.

(67) Walrafen, W.F., "Water a Comprehensive Treatise", Frank F. eds. Plenum Press, N.Y., Chapter 5 (1972).

(68) Breniga,W.; Romanb, T., Chem. Phys. 2014, 439, 117-120.

Figure Captions

Figure 1. (Color online). Structures and geometrical parameters of neutral water clusters, dimer (*n*=2), trimer (*n*=3), and tetramer (*n*=4). Bond lengths (in Å) were calculated at the MP2 and CCSD/6-311++G(d,p) levels. Spatial distributions of spin orbital of water radical cations at vertical ionization point were calculated at the MP2/6-311++G(d,p) level.

Figure 2. (Color online). Snapshots of water trimer cation $(H_2O)_3^+$ after vertical ionization from optimized structure. The values are bond distance in Å.

Figure 3. (Color online). Snapshots of water tetramer cation $(H_2O)_4^+$ after vertical ionization from optimized structure. The values are bond distance in Å.

Figure 4. (Color online). Time evolutions of (A) potential energy and (B) geometrical parameters of water tetramer cation $(H_2O)_4^+$ following the vertical ionization.

Figure 5. (Color online). Reaction time for the proton transfer in water tetramer cation plotted as a function of run number of trajectory.

Figure 6. (Color online). Optimized structures of water cluster radical cations $(H_2O)_n^+$ (*n*=2, 3, and 4). Upper and lower values indicate relative energies (in kcal/mol) of $(H_2O)_4^+$ calculated by MP2 and CCSD methods with 6-311++G(d,p) basis set, respectively.

Figure 7. (Color online). Energy diagram of ionization process of water clusters $(H_2O)_n$ (*n*=2, 3, and 4).

Figure 8. (Color online). (left) Superimposes of snapshots for the first proton transfer process, and (right) potential energy curve for the proton transfer process calculated by static ab-initio calculation (MP2/6-311++G(d,p) level). The values obtained by direct AIMD calculation are given as filled circle.

Figure 9. (Color online). Time evolution of oxygen-oxygen (O-O) bond distances of neutral water tetramer at 10 K. Time is in atomic unit. Calculation was carried out at the B3LYP/6-311++G(d,p) level.

Table 1. Molecular charges and spin densities on H_2O in neutral and cationic water clusters $(H_2O)_n$ and $(H_2O)_n^+$ (n=2-4). Structures of $(H_2O)_n^+$ (n=2-4) were located in the vertical ionization points from the parent water clusters. The values were calculated at the MP2/6-311++G(d,p) level. Notation "ver" means vertical ionized state from parent neutral water cluster.

		W1	W2	W3	W4
charge	n=2(0)	0.02	-0.02		
	n=3(0)	0.00	0.00	0.00	
	n=4(0)	0.00	0.00	0.00	0.00
	n=2(+)ver	0.95	0.05		
	n=3(+)ver	0.91	0.07	0.02	
	n=4(+)ver	0.89	0.08	0.03	0.01
spin density	n=2(+)ver	1.00	0.00		
	n=3(+)ver	0.99	0.00	0.01	
	n=4(+)ver	1.00	0.00	0.00	0.01

Table 2. Reaction time (in fs) of proton transfer in water cluster cations $(H_2O)_n^+$ (n=2-4) after the ionization.

Proton transfer	n=2	3	4
1st	28.4	15.1	9.9
2nd		119.6	39.6
3rd		143.1	49.5
4th			63.4

Table 3. Vertical ionization energies of $(H_2O)_n$ (*n*=2-4) (*Ip* in eV), stabilization energies of complex of radical cation of $(H_2O)_n^+$ (ΔE_{stable} in kcal/mol), dissociation energies of OH radical from $(H_2O)_n^+$ (ΔE_{diss} in kcal/mol), and available energies of OH dissociation reaction (ΔE_{avail} in kcal/mol).

$(H_2O)_n$	method	ΔE_{stable}	ΔE_{diss}	ΔE_{avail}	Ip
n=2	MP2	21.5	22.3	-0.8	11.7
	CCSD	21.5	21.5	0.0	11.4
n=3	MP2	52.9	37.6	15.3	12.3
	CCSD	52.0	37.0	15.0	12.0
n=4	MP2	55.4	7.9	47.5	12.2
	CCSD	60.3	12.9	47.4	11.9

Figure 1.

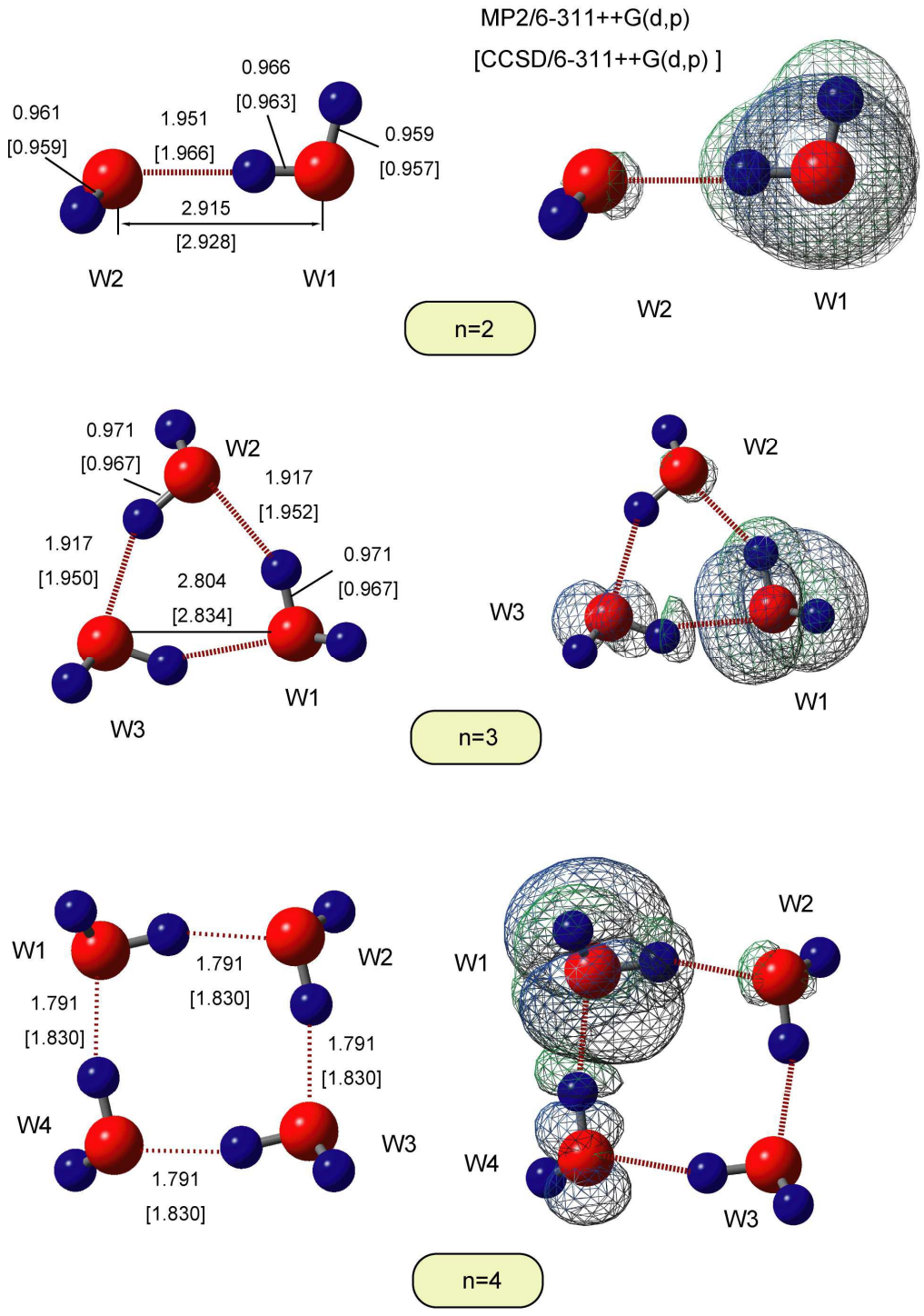

Figure 2.

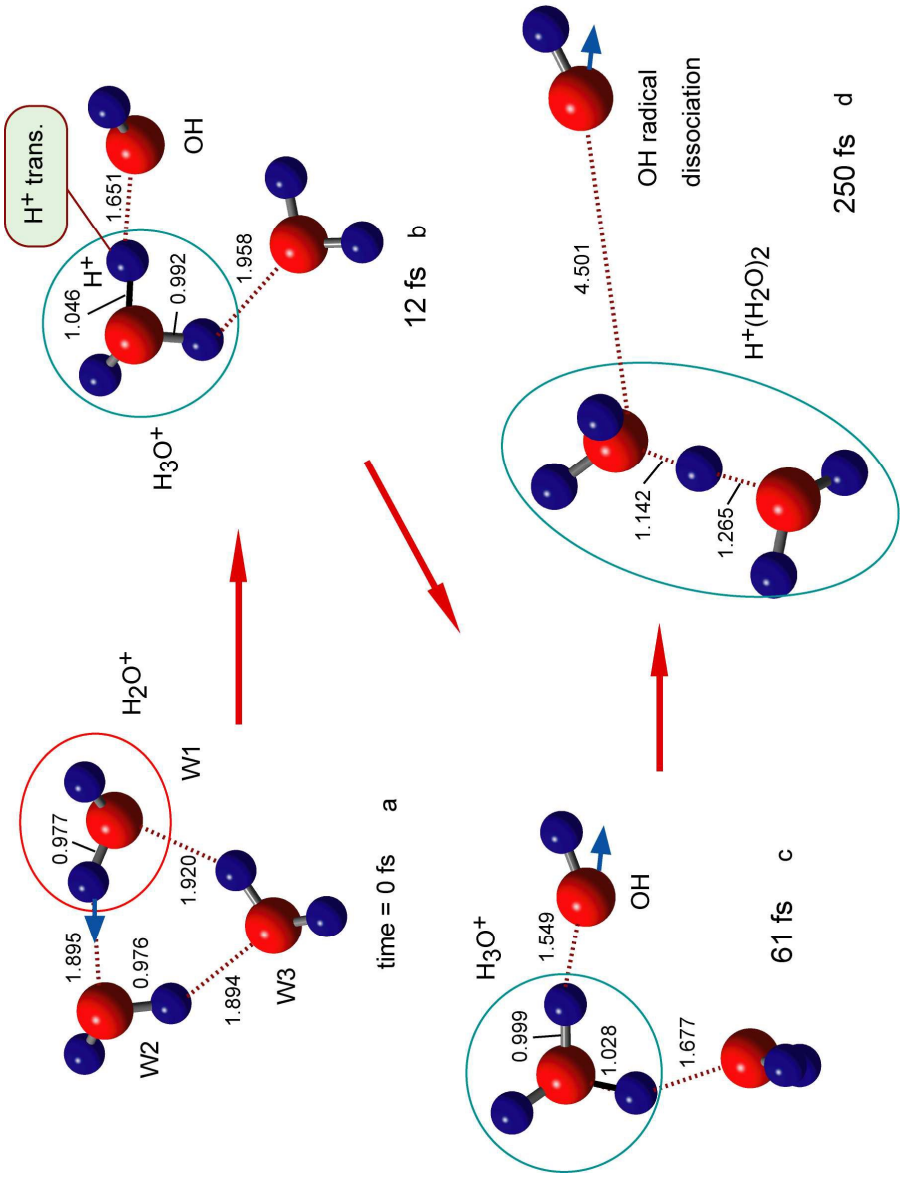

Figure 3.

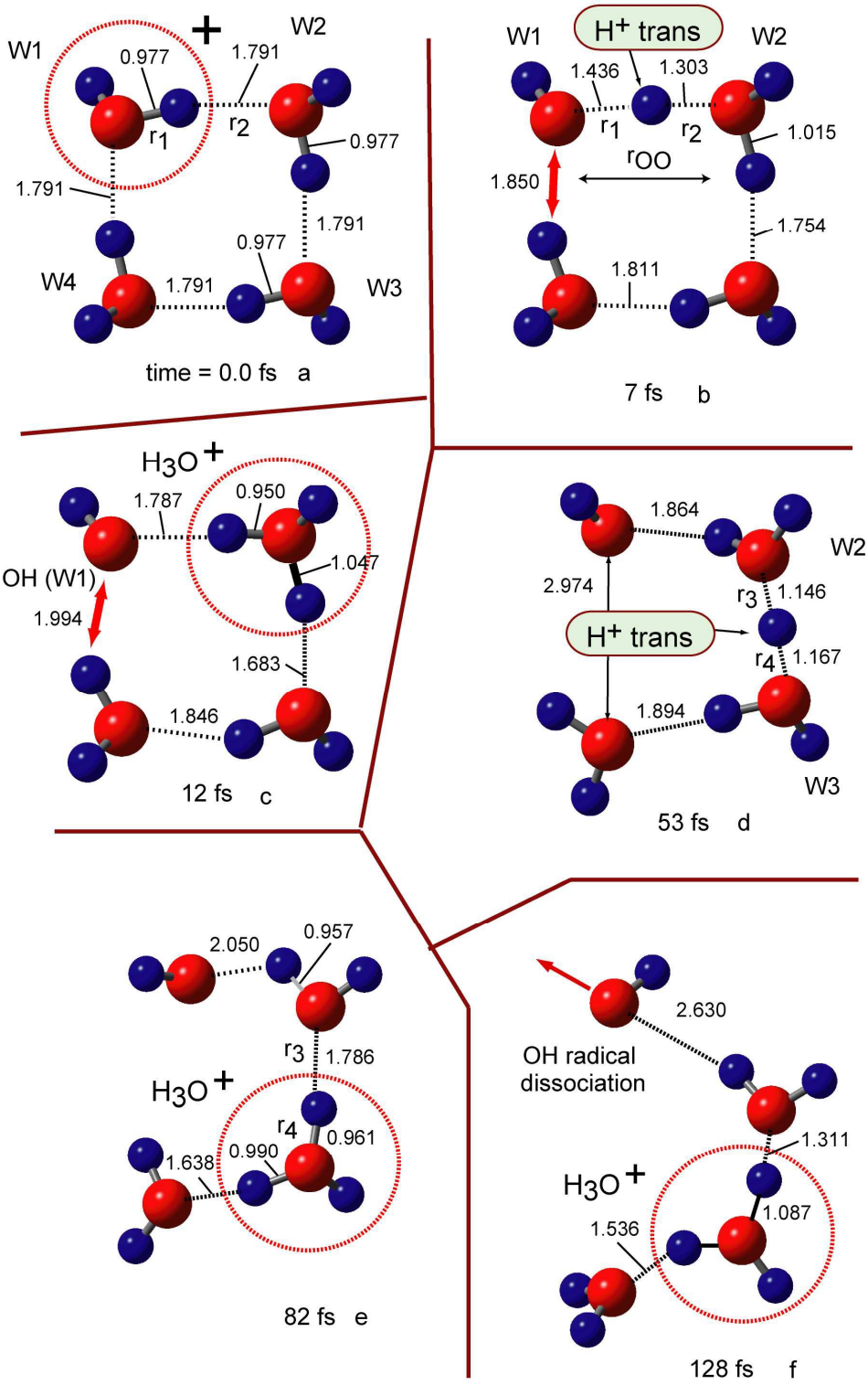

Figure 4.

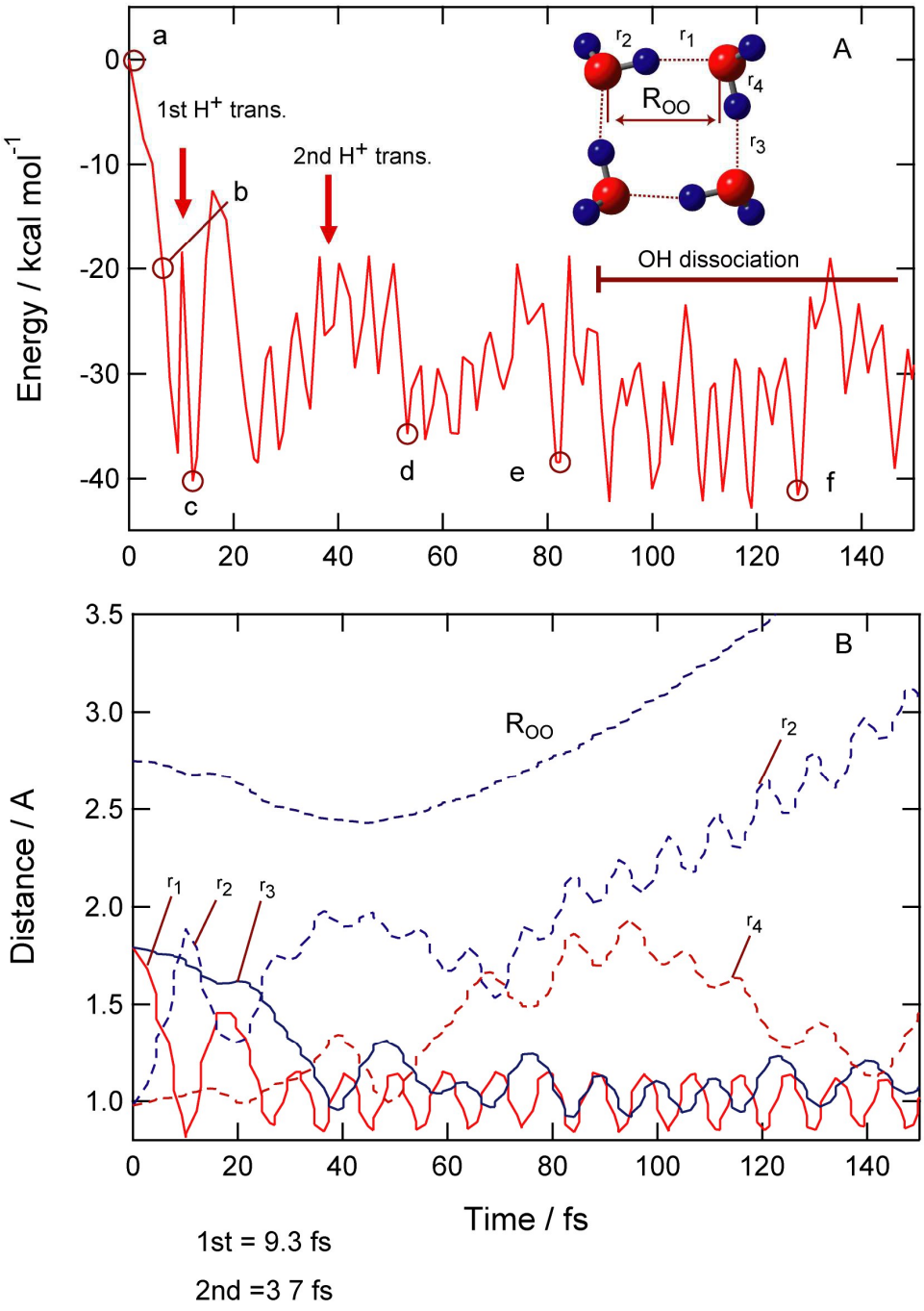

Figure 5.

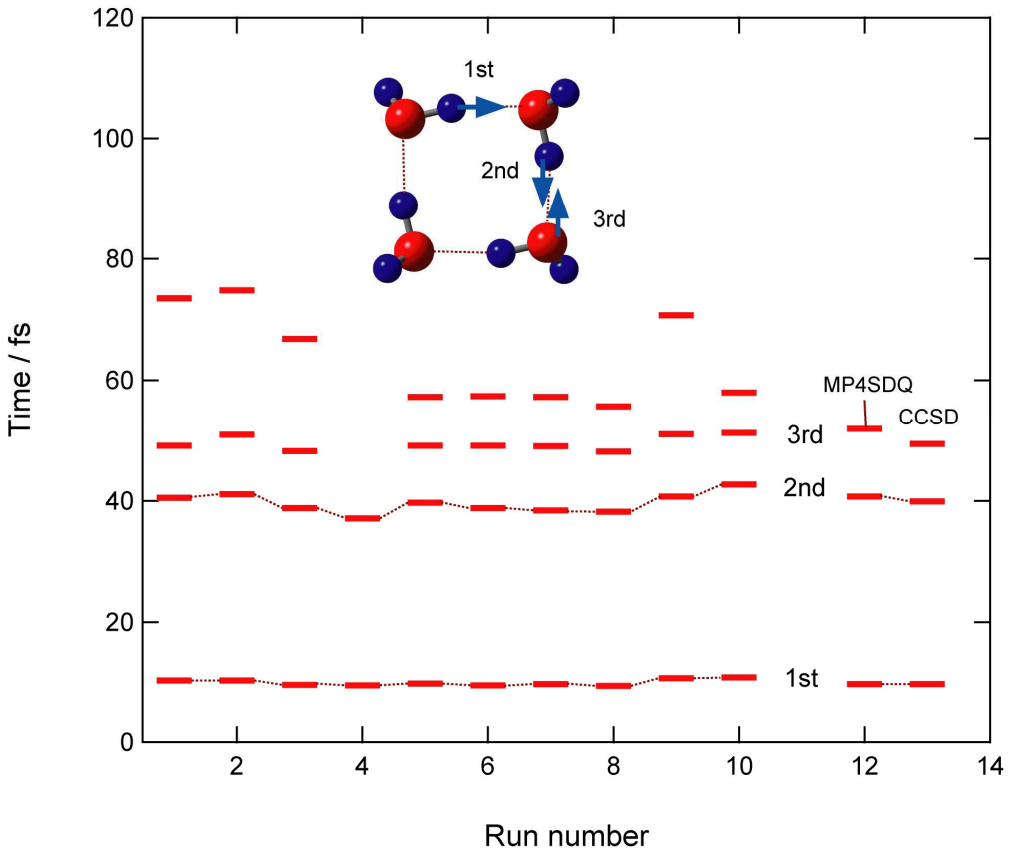

Figure 6.

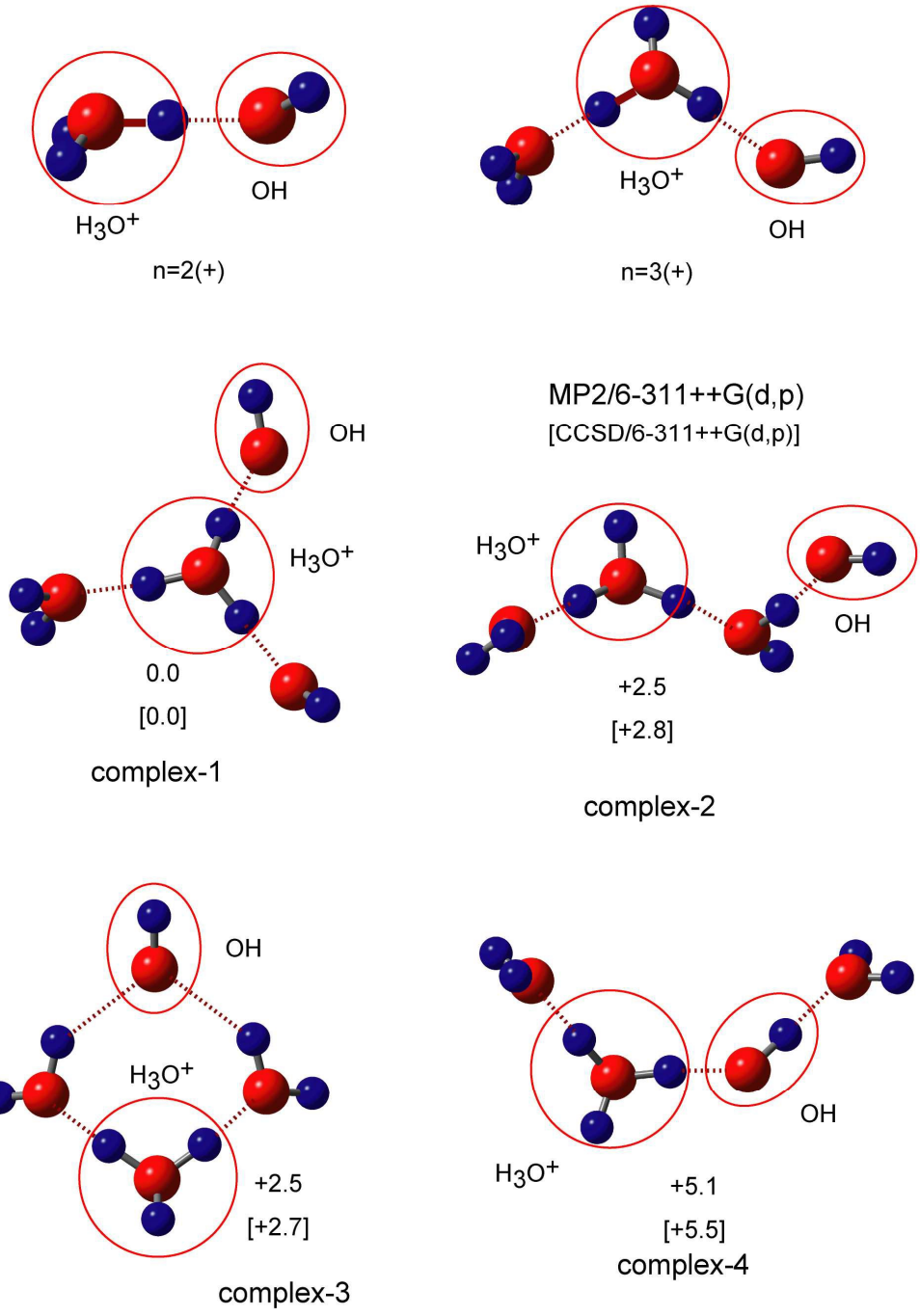

Figure 7.

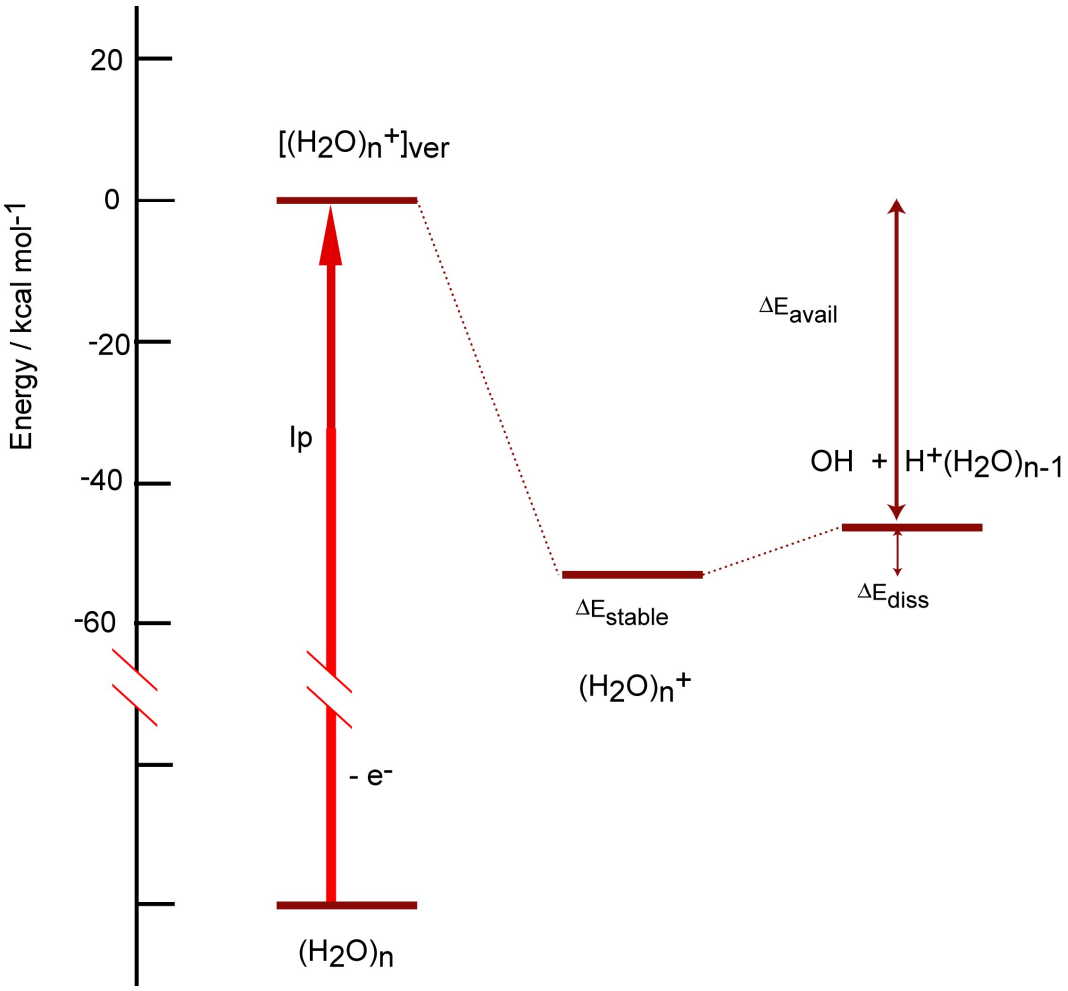

Figure 8.

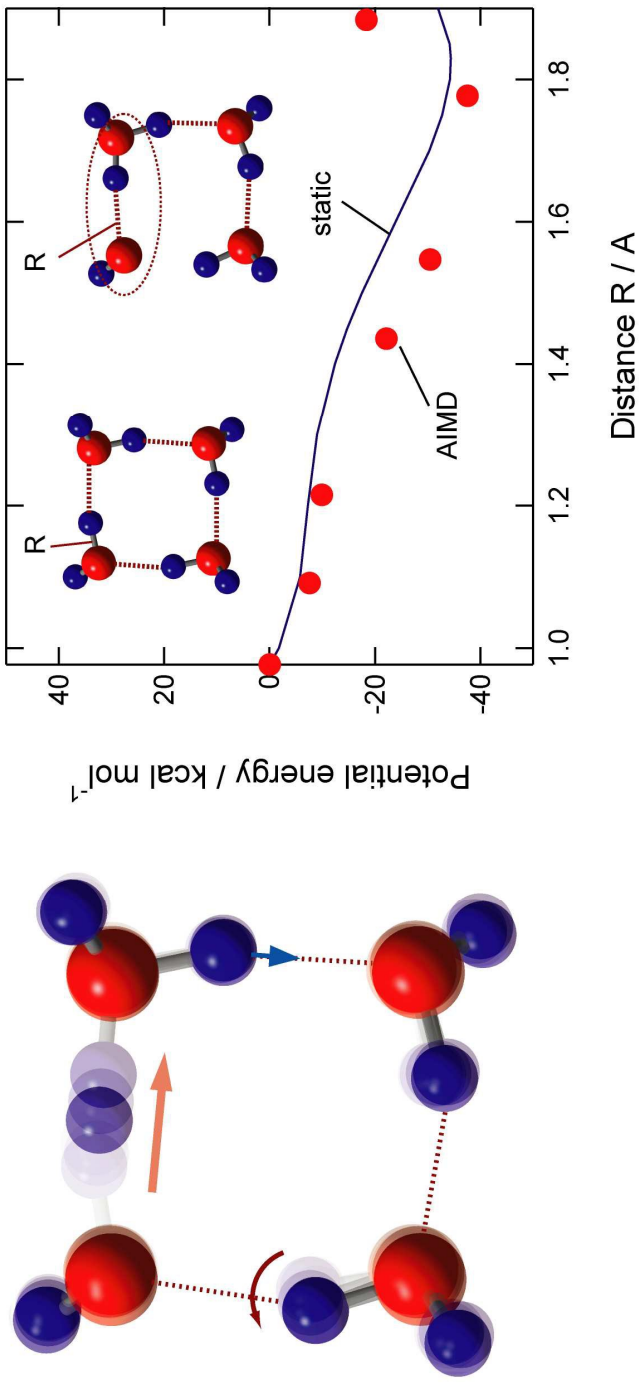

Figure 9.